Prospect Theoretic Utility Based Human Decision Making in Multi-Agent Systems

Baocheng Geng , Swastik Brahma , *Member, IEEE*, Thakshila Wimalajeewa , *Senior Member, IEEE*, Pramod K. Varshney , *Life Fellow, IEEE*, and Muralidhar Rangaswamy , *Fellow, IEEE*

Abstract—This paper studies human decision making via a utility based approach in a binary hypothesis testing framework that includes the consideration of individual behavioral disparity. Unlike rational decision makers who make decisions so as to maximize their expected utility, humans tend to maximize their subjective utilities, which are usually distorted due to cognitive biases. We use the value function and the probability weighting function from prospect theory to model human cognitive biases and obtain their subjective utility function in decision making. First, we show that the decision rule which maximizes the subjective utility function reduces to a likelihood ratio test (LRT). Second, to capture the unreliable nature of human decision making behavior, we model the decision threshold of a human as a Gaussian random variable, whose mean is determined by his/her cognitive bias, and the variance represents the uncertainty of the agent while making a decision. This human decision making framework under behavioral biases incorporates both cognitive biases and uncertainties. We consider several decision fusion scenarios that include humans. Extensive numerical results are provided throughout the paper to illustrate the impact of human behavioral biases on the performance of the decision making systems.

Index Terms—Utility based hypothesis testing, behavioral bias, prospect theory, human decision making, information fusion, decision fusion.

I. INTRODUCTION

ISTRIBUTED sensor networks for information fusion and inference have been studied quite extensively due to their wide applications in security, defense, environmental monitoring and in almost all intelligent systems [1]–[3]. Sensor nodes can be programmed to take measurements regarding a phenomenon of interest (PoI), and to transmit their quantized and/or compressed sensing data to a fusion center (FC). In many

Manuscript received May 25, 2019; revised November 27, 2019; accepted January 20, 2020. Date of publication January 30, 2020; date of current version February 14, 2020. The associate editor coordinating the review of this manuscript and approving it for publication was Prof. Marco Moretti. This work was supported in part by the DDDAS program of AFOSR, under Grant FA9550-17-0313 and in part by the NSF under Grants ENG 1609916 and HRD 1912414. (Corresponding author: Baocheng Geng.)

- B. Geng and P. K. Varshney are with the Department of Electrical Engineering and Computer Science, Syracuse University, Syracuse, NY 13205 USA (e-mail: bageng@syr.edu; varshney@syr.edu).
- S. Brahma is with the Department of Computer Science, Tennessee State University, Nashville, TN 37209 USA (e-mail: sbrahma@Tnstate.edu).
- T. Wimalajeewa is with the BAE Systems, Burlinton, MA 01803 USA (e-mail: thakshila.wimalajeewa@ieee.org).
- M. Rangaswamy is with the Air Force Research Labs, Wright-Patterson Air Force Base, Dayton, OH 45433 USA (e-mail: muralidhar.rangaswamy@us.af.mil).

Digital Object Identifier 10.1109/TSP.2020.2970339

situations, these nodes act as local decision makers that assist the FC in making an inference regarding the state of the PoI. When we have physical sensors serving as local decision makers, the optimal decision rules for both the local decision makers and the FC for different cases have been derived in the literature (see, for e.g., [1], [2], [4], [5]). However, in many emerging applications, such as crowdsourcing, humans have become an essential part of the decision making process. In fact, in many applications humans serve as 'sensors' who contribute information towards an inference task. Examples of human sensors include members of a committee or an organization, and scouts monitoring a phenomenon to gather intelligence. In addition, posts on Twitter and ratings on recommendation websites such as Yelp can also be regarded as decisions made by human agents, which can be aggregated for obtaining inferences. Unlike traditional physical sensors that provide objective measurements towards a distributed inference task, humans are subjective in expressing their opinions or decisions.

The difficulty in modeling human decision making arises because of their cognitive biases as well as due to the uncertainties exhibited by human decision makers. Cognitive biases are characterized by diminishing marginal utility, risk seeking/aversion behavior and loss aversion attitude; while the uncertainties in decision making behavior of humans can arise from emotion, time constraint, fatigue and operating environment [6]–[9]. The purpose of this work is to develop a unified framework that incorporates both cognitive biases and uncertainties in decision making, which we call decision making under behavioral biases. We begin our study with the discussion of cognitive biases based on prospect theory (PT). This Nobel-prize-winning theory proposed by Kahneman and Tversky [6] provides a theoretically sound description of human cognitive biases through a value function and a probability weighting function. Value function, as the name suggests, acts on the values (gains and losses) to reflect humans' loss attitude, i.e., asymmetric valuation towards gains and losses. From the cognitive psychology viewpoint, people are usually loss averse in the sense that loss feels worse than the gain of an equivalent amount feels good. Probability weighting function, on the other hand, acts on the probability that an event will occur. It represents the fact that in humans' cognitive perception, they usually overweigh small probabilities and underweigh large probabilities.

This paper considers human decision making behavior in the context of hypothesis testing. As is well known, humans make decisions in the framework of hypothesis testing and the decision

1053-587X © 2020 IEEE. Personal use is permitted, but republication/redistribution requires IEEE permission. See https://www.ieee.org/publications/rights/index.html for more information.

is made by selecting the hypothesis that best supports the given set of observations [10]. There have only been a few works that incorporate PT into hypothesis testing to model human decision making. In [11], Nadendla *et al.* applied prospect theory to hypothesis testing and analyzed the behavior of optimists and pessimists of different types. In their work, the definitions of optimists and pessimists were limited in scope for modeling general human behavior. As a result, the analysis cannot be extended to the development of explicit decision rules for agents with arbitrary prospect theoretic parameters. The optimality of the likelihood ratio test (LRT), which is known to be the optimal decision rule in minimizing the Bayesian risk, was investigated in PT based hypothesis testing in [12]. The authors showed that the LRT may or may not be optimal for behavioral decision makers under the Neyman-Pearson criterion.

In addition to being subject to cognitive biases, human agents may also exhibit uncertainties in decision making. There have been some research efforts that explore uncertainties in human decision making. Since human participants have different backgrounds and expertise regarding a PoI, the qualities of the local decisions vary quite considerably. It was shown in [13] that when there is no reliability information available for each decision maker, the majority rule is often the choice that gives better results in group decision making, compared to other criteria such as the consensus rule. Budescu et al. [14] showed a scenario where the FC gives more weight to the decisions made by agents who have been more accurate in the past, while it assigns less weight to the decisions made by unreliable agents. In [15], the fusion of local decisions made by humans was analyzed using signal detection techniques. The authors studied how the quality variation of local decisions affects the decision performance of the FC. Meanwhile, there have been research efforts which attempt to model human decision uncertainties in different contexts. The quantization of prior probabilities in a Bayesian decision making framework was analyzed to model categorization in human decision making [16]. Vempaty et al. [17] constructed a Bayesian hierarchical structure to model human decision making behavior at individual level, crowd level and population level. In [18], Wimalajeewa et al. studied collaborative human decision making and assumed that each participating agent makes decisions using a random decision threshold. The authors in [19] investigated the conditions under which integration of human operators with physical sensors can improve the performance in binary decision making. A novel sequential paradigm for crowdsourced classification considering limited knowledge of human worker's reliability was presented in [20].

In the above works that study cognitive biases in the context of decision making [11], [12], the authors assume that humans make decisions so as to minimize their behavioral Bayesian risk under the Bayesian formulation. However, psychology studies show that in practice, instead of employing the decision rule that minimizes the behavioral Bayesian risk, people use utility based approaches based on existing evidence and select the action which results in the highest expected payoff over all possible alternatives [21], [22]. To the best of our knowledge, the analysis of human decision making from a utility based perspective while

considering cognitive biases under PT has not been addressed in the previous literature. Besides, the existing work has not considered how the uncertainties differ from one human to another in decision making, i.e., the individual level quantification of human uncertainty. No prior work has discussed the combination of both decision uncertainties and cognitive biases in affecting the decision quality. Such a unified framework is crucial to the design of efficient decision rules when we have humans-in-the-loop, and is relevant in many areas such as situational awareness in monitored civil and military systems, targeted advertising and recommendation systems, portfolio management, insurance policy design, as well as investment in financial markets.

The main objective of this work is to investigate the impact of behavioral biases that include cognitive biases and decision uncertainties on human decision making and, correspondingly, on the decision fusion rule in multi-agent systems. Specifically, our contributions are:

- We consider that a human perceives the utility of making correct decisions to be gain and perceives the utility of making wrong decisions to be loss. Value functions and probability weighting functions based on PT are exploited to construct the subjective utility function for humans in a binary hypothesis testing problem. The optimal decision rule for cognitively biased humans is determined in which they choose the hypothesis that maximizes their subjective expected utility.
- Next, we consider that humans use a threshold based scheme to make decisions based on their observations [18], [23]. The threshold of a human is treated as a random variable where the threshold mean is determined by the person's cognitive biases under PT, and the threshold variance represents the person's uncertainty in decision making. We thoroughly study the impact of an individual's behavioral biases (cognitive biases and uncertainties) on the performance of decision making systems that involve human participation. In particular, three configurations are investigated: (i) a human acts as an assistant to help a rational FC make the final decision, (ii) the other scheme considers the FC to be a behaviorally biased human who makes the final decision with the help of a physical sensor, and (iii) two-person decision fusion, where two human agents independently provide their local decisions to the FC.
- Finally, we investigate collaborative human decision making and obtain the optimal decision fusion rule at the FC. In our work, the FC is able to adjust its decision making strategy when the human behavioral properties change. This provides generality and flexibility compared to existing group decision fusion schemes, such as those developed in [13], [15], [24], [25], where the authors did not consider the behavioral biases of human participants.

¹When the humans make right decisions, there is a potential gain as they have a better knowledge of the status of the environment and remedial actions can be taken. On the other hand, when humans make wrong decisions in terms of false alarms and miss detections, there is a loss as they have an inaccurate perception regarding the PoI.

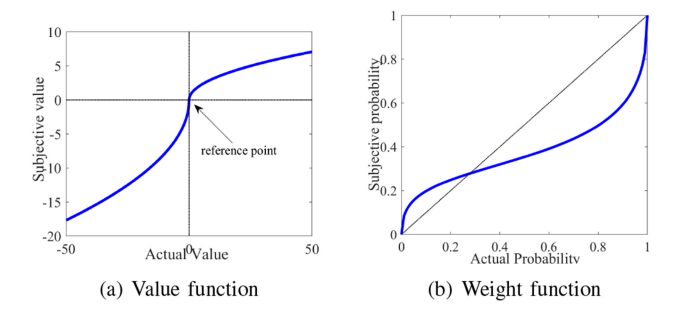


Fig. 1. Illustration of the value function and the weight function in prospect theory.

The rest of the paper is organized as follows. In Section II, we provide some background of PT and introduce the utility based hypothesis testing framework. Cognitive biases and uncertainties are incorporated to model human decision making. In Section III, three different decision making problems involving human participation are investigated: humans act as agents in assisting the FC to make the final decision, a human acts as the FC and decision fusion of two human agents. We further study collaborative human decision making in Section IV and conclude our work in Section V.

II. UTILITY BASED HYPOTHESIS TESTING

In this section, we explore human decision making for binary hypothesis testing problems using utility based decision theory, starting with a brief introduction of prospect theory.

A. Prospect Theory Background

From a psychology viewpoint, people are said to be loss averse in the sense that they feel more hurt when they lose something, than they feel good when they gain something of equal value. For example, the satisfaction a person gets when \$100 is added to his/her present value is less than the loss of satisfaction when \$100 is subtracted from the present value. In prospect theory [6], the value function v(x) plotted in Fig. 1(a) characterizes the loss aversion effect by assigning a subjective utility to an outcome x:

$$v(x) = \begin{cases} x^{\lambda} & x \ge 0\\ -\beta(-x)^{\lambda} & x < 0 \end{cases}$$
 (1)

where x is the actual gain (when it is positive) or loss (when it is negative), and v(x) represents the human subjective valuation of x. Utilities under PT are perceived as gains and losses with respect to a reference point, which is a subjective value above which utilities are perceived as gains and utilities blow which are perceived as losses. With different reference points, the characterization of human behavior even for the same experiment is significantly different. In this work, for simplicity, we assume the case where the gain and loss are perceived with respect to the fixed reference point set at zero so that positive utilities humans derive from deciding correctly correspond to gains and negative utilities humans derive from deciding incorrectly correspond to losses. β is the loss aversion coefficient, and v(x) reflects

people's different loss aversion attitudes that are realized by the variation of parameter β . When a person becomes more loss averse, β increases and the subjective valuation of a fixed loss appears to be more significant. λ characterizes the phenomenon of diminishing marginal utility, which indicates that as the total number of units of gain (or loss) increases, the utility of an additional unit of gain (or loss) to a person decreases. This effect can be seen in Fig. 1(a) as the curve saturates when it goes in either direction (positive or negative).

On the other hand, the probability weighting function reflects people's four-fold pattern of risk attitudes, i.e., risk-seeking for small-probabilistic gains and large-probabilistic losses, and riskaversion for small-probabilistic losses and large-probabilistic gains. This phenomenon can be interpreted as people overweighing small probabilities and underweighing large probabilities. For example, the certainty effect, which states that a sure gain is favored over a probabilistic gain, indicates humans' risk aversion behavior for large probabilistic gains. Tversky and Kahneman [6] illustrated the certainty effect by investigating which of the following options do people prefer: (A) a sure gain of \$30; and (B) 80% chance to win \$45 and 20% chance to win nothing. In this case, most participants chose option A and it demonstrates the typical risk-aversion phenomenon in PT because the expected value of option B ($\$45 \times 0.8 = \36) exceeds that of A by 20%. A detailed discussion of the four-fold pattern of risk behavior can be found in [26].

As shown in Fig. 1(b), the probability weighting function in PT is:

$$w(p) = \frac{p^{\alpha}}{(p^{\alpha} + (1-p)^{\alpha})^{1/\alpha}}$$
 (2)

where p is the actual probability with which an event occurs. w(p) gives the subjective probability distorted by the probability distortion coefficient α . For behaviorally unbiased people, $\alpha=1,\,\beta=1$ and $\lambda=1$. In a landmark study [26], the authors conducted experiments by letting human subjects choose the preference between a series of prospect pairs. Based on the experimental data, the behavioral parameters $\alpha,\,\beta$ and λ of each individual can be estimated using a nonlinear regression procedure. According to their result, the medians of $\alpha,\,\beta$ and λ are 0.69, 2.25 and 0.88, respectively.

B. Decision Making Model and Bayesian Formulation Under PT

In hypothesis testing, an agent makes a decision on which of the hypothesis H_0 or H_1 is true, based on an observation r regarding a PoI. The observations under the two hypotheses are $H_0: r=s_0+w,\ H_1: r=s_1+w,$ where s_0 and s_1 are signal amplitudes under H_0 and H_1 , respectively, and w denotes the observation noise. Assume that the signal and noise are independent of each other and the probability density functions (PDFs) of r under H_0 and H_1 are assumed to be known. We denote them as $f_0(r)$ and $f_1(r)$, respectively. The prior probabilities of H_0 and H_1 are π_0 and π_1 , respectively. Let C_{ij} be the cost of declaring H_i when H_j is true for $i,j\in\{0,1\}$. These costs are assigned to reflect the the relative importance of the four courses of actions [1], [27].

Let \mathcal{R} be the acceptance region of hypothesis H_1 , then the decision maker employs the following decision rule:

$$d = \begin{cases} 1; & \text{if } r \in \mathcal{R} \\ 0; & \text{otherwise} \end{cases}$$
 (3)

When human cognitive biases are modeled by PT, i.e., the costs and probabilities are affected by the value function and the probability weighting function, respectively, the expected behavioral risk under Bayesian formulation is:

$$b(\mathcal{R}) = \sum_{i=0}^{1} \sum_{j=0}^{1} w[Pr(\text{Declare } H_i | H_j \text{ is true})] \cdot v(C_{ij}).$$

The objective is to find the optimal acceptance region \mathcal{R}^* that minimizes the behavioral risk:

$$\mathcal{R}^* = \arg\min_{\mathcal{R} \in \mathbb{R}} \ b(\mathcal{R}). \tag{4}$$

Because of the nonlinearity of the value function (1) and the probability weighting function (2), the Bayesian formulation of the optimization problem (4) does not have an explicit solution [11], [12]. Under Bayesian formulation, the decision rule, i.e., the acceptance region of hypothesis H_1 , is pre-determined before any observation is received. Whenever an observation comes in, a decision is made according to the same decision rule. However, psychology studies suggest that humans make decisions after observing some evidence, where the observation provides some support for a hypothesis. Depending on whether the observation confirms or refutes a hypothesis, human confidence towards a hypothesis can vary continuously from 100% certainty about its truth to 100% certainty about its falsity. Correspondingly, when making a decision, a rational decision maker calculates the expected utility of deciding each alternative hypothesis based on observed evidences, and selects the one that results in the highest expected utility [10], [21], [22]. This action of the rational decision makers is called decision making under the expected utility theory (EUT) framework [28]. We proceed with the above utility based methods to model human decision making and employ PT to incorporate human cognitive biases. In fact, when a rational decision maker selects the hypothesis from a set of alternative hypotheses that results in the maximum expected payoff under EUT, it is equivalent to the decision rule that minimizes the Bayesian cost [29], [30]. However, in the following, we will show that this equivalence does not hold in general when the decision maker is cognitively biased under PT.

C. Subjective Utility Based Hypothesis Testing

We begin with the analysis of utility based decision making for binary hypothesis testing under EUT, where the decision makers are assumed to be rational. Instead of minimizing the Bayesian risk (4), the objective is to choose the hypothesis that results in the highest expected utility. Let U_{ij} denote the utility of deciding H_i when the true hypothesis is H_j , for $i,j \in \{0,1\}$. Thus, U_{00} and U_{11} represent the utilities of correct decisions and are usually positive, while U_{10} and U_{01} represent the utilities of wrong decisions and are usually negative. Given an observation r, a rational decision maker's expected utility of declaring H_0

and H_1 are:

$$\begin{aligned} \mathbf{EU}(\text{Declare } H_0) &= \Pr(H_0|r)U_{00} + \Pr(H_1|r)U_{01} \\ \mathbf{EU}(\text{Declare } H_1) &= \Pr(H_0|r)U_{10} + \Pr(H_1|r)U_{11}, \quad (5) \end{aligned}$$

where $Pr(H_i|r)$ denotes the probability that H_i is true given that the observation is r, and

$$Pr(H_i|r) = \frac{f(r|H_i)\pi_i}{f(r)} = \frac{f_i(r)\pi_i}{f(r)}$$
(6)

for i=0,1, respectively, where $f(\cdot)$ and $f_i(\cdot)$ denote the appropriate PDFs and π_i is the prior probability of hypothesis H_i . Given the observation r, the hypothesis H_0 or H_1 whichever has a larger expected utility is declared to be true

$$\mathbf{EU}(\text{Declare } H_1) \overset{H_1}{\underset{H_0}{\geq}} \mathbf{EU}(\text{Declare } H_0). \tag{7}$$

Substitute the expression of $Pr(H_i|r)$ given in (6) into (5)

$$\mathbf{EU}(\text{Declare } H_0) = \frac{f_0(r)\pi_0}{f(r)} U_{00} + \frac{f_1(r)\pi_1}{f(r)} U_{01}$$

$$\mathbf{EU}(\text{Declare } H_1) = \frac{f_0(r)\pi_0}{f(r)}U_{10} + \frac{f_1(r)\pi_1}{f(r)}U_{11}$$

Next, we substitute the above equations into (7), and the utility based decision rule reduces to the classical LRT:

$$\frac{f_1(r)}{f_0(r)} \stackrel{\stackrel{H_1}{\geq}}{\underset{H_0}{\geq}} \frac{\pi_0(U_{00} - U_{10})}{\pi_1(U_{11} - U_{01})} \stackrel{\triangle}{=} \eta.$$
 (8)

which is also the optimal decision rule that minimizes the Bayesian cost.

In the statistical detection theory framework, the decision making agent is assumed to be rational and the objective is to maximize the expected utility. Under EUT, decision makers are rational in the sense that they are able to calculate the expected utility of each action without biases. For example, a typical characteristic of rational decision makers is that they should be indifferent between two alternative courses of action if their expected utilities are the same. However, due to human cognitive biases in perceiving the utilities and the probabilities, a human usually prefers a sure gain over a probabilistic gain even if the two alternatives have the same expected utility. In many settings when the decisions are made by humans, certain behavioral factors may cause the results to deviate from the outcomes predicted by EUT. Unlike rational decision makers who choose the hypothesis that maximizes their expected utilities, humans act to maximize their subjective utilities under cognitive biases. When calculating the subjective utility of declaring H_0 and H_1 , we employ PT by applying the value function $v(\cdot)$ defined in (1) on the utilities and applying the probability weighting function $w(\cdot)$ defined in (2) on the probabilities. Given observation r, the subjective utilities of declaring H_0 and H_1 are:

SU(Declare
$$H_0$$
) = w (Pr($H_0|r$)) $v(U_{00}) + w$ (Pr($H_1|r$)) $v(U_{01})$

SU(Declare
$$H_1$$
) = w (Pr($H_0|r$)) $v(U_{10}) + w$ (Pr($H_1|r$)) $v(U_{11})$.

Without optimizing over all possible events in a Bayesian sense, humans are known to select the alternative which has a higher subjective utility after receiving observation r:

$$\mathbf{SU}(\text{Declare } H_1) \overset{H_1}{\underset{H_0}{\geq}} \mathbf{SU}(\text{Declare } H_0).$$
 (10)

Combining (9) and (10), the subjective utility based decision rule becomes:

$$\frac{w\left(\Pr(H_1|r)\right)}{w\left(\Pr(H_0|r)\right)} \stackrel{H_1}{\underset{H_0}{\geq}} \frac{v(U_{00}) - v(U_{10})}{v(U_{11}) - v(U_{01})} \triangleq \frac{V_{00} - V_{10}}{V_{11} - V_{01}}, \quad (11)$$

where $V_{00}, V_{01}, V_{10}, V_{11}$ are the subjective utilities when the value function (1) acts on $U_{00}, U_{01}, U_{10}, U_{11}$, respectively. Again, V_{00} and V_{11} are positive, while V_{01} and V_{10} are negative. Employing the expression of the weight function given in (2) and the expression of $Pr(H_i|r)$ given in (6), and noting that $Pr(H_1|r) = 1 - Pr(H_0|r)$, we have $\frac{w(Pr(H_1|r))}{w(Pr(H_0|r))} = \frac{Pr(H_1|r)^{\alpha}}{Pr(H_0|r)^{\alpha}}$. It follows that the decision rule given in (11) becomes

$$\frac{f_1(r)}{f_0(r)} \stackrel{H_1}{\underset{H_0}{\geq}} \left(\frac{V_{00} - V_{10}}{V_{11} - V_{01}}\right)^{\frac{1}{\alpha}} \frac{\pi_0}{\pi_1} \triangleq \eta_p. \tag{12}$$

Thus, the test reduces to a LRT with threshold η_p as stated in the following theorem.

Theorem 1: Under prospect theoretic framework, the optimal subjective utility based decision rule reduces to an LRT. The threshold of the LRT, η_p , is a monotonous function of parameters α and β .

In many applications, the likelihood ratio $\lambda(r) = \frac{f_1(r)}{f_0(r)}$ is strictly increasing or decreasing with respect to r. One example is when $f_1(r)$ and $f_0(r)$ are Gaussian PDFs with different means and the same variance. Gaussian distributions are very commonly used as they characterize a large number of problems in signal processing and communications. In this case, the LRT reduces to a threshold based decision rule based on the observation r and the optimal decision threshold t is monotone with respect to α and β as well.

Proposition 1: When the likelihood ratio $\Lambda(r)$ is strictly increasing or decreasing, the LRT in (12) becomes a threshold decision rule. The optimal decision threshold is monotone with respect to behavioral parameters α and β , respectively.

Proof: Given the monotonicity of $\Lambda(r)$, the likelihood ratio test (12) is equivalent to $r \gtrsim_{H_0}^{H_1} t_0$ or $r \gtrsim_{H_1}^{H_0} t_0$, depending on whether $\Lambda(r)$ is increasing or decreasing. The decision threshold t_0 is obtained by setting $t_0 = \Lambda^{-1}(\eta_p)$, where $\Lambda^{-1}(\cdot)$ is the inverse function of $\Lambda(r)$. Because of the monotonicity of $\Lambda^{-1}(\cdot)$, t_0 is monotonous with respect to η_p . From Theorem 1, we know that η_p is a monotonous function with respect to parameters α and β , it follows that t_0 is monotonous with respect to α and β as well.

 $^2 \text{In case that } f_1(r) \text{ and } f_0(r) \text{ are Gaussian PDFs with means } m_1 \text{ and } m_0,$ and variance $\sigma_s^2, \ \Lambda(r) = \frac{f_1(r)}{f_0(r)} = e^{\frac{2(m_1-m_0)r-(m_1^2-m_0^2)}{2\sigma_s^2}},$ which is strictly increasing if $m_1 > m_0$, and strictly decreasing if $m_1 < m_0$.

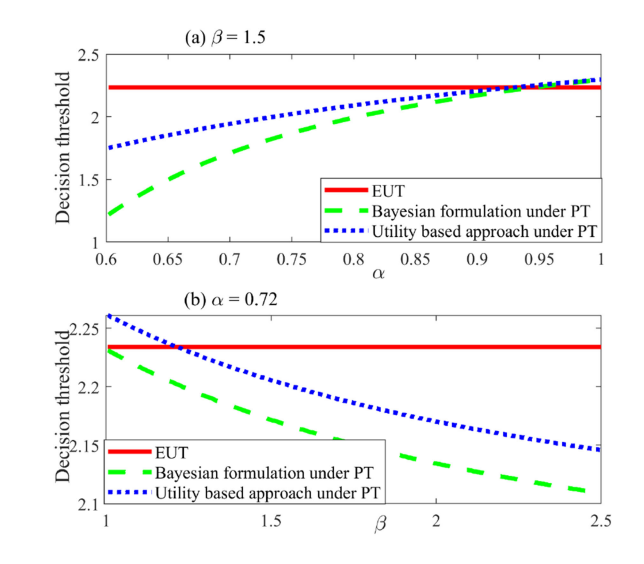


Fig. 2. Decision thresholds with respect to behavioral parameters.

In the remainder of this paper, we consider human decision making for the binary hypothesis testing problem, and the observations under each hypothesis are assumed to follow a Gaussian distribution:

$$H_0: r \sim \mathcal{N}(m_0, \sigma_s^2)$$

$$H_1: r \sim \mathcal{N}(m_1, \sigma_s^2)$$
(13)

where the signal means under H_0 and H_1 are m_0 and m_1 , respectively. The signal variance under both hypotheses is σ_s^2 . We assume that $m_0 < m_1$ and the diminishing marginal utility parameter λ from PT is set equal to 0.88. We focus on analyzing how behavioral parameters α and β affect the human decision qualities.

For illustration, we conduct experiments on a hypothesis testing problem with the following setting: $\pi_0 = 0.7, \pi_1 =$ $0.3, U_{11} = U_{00} = 20, U_{01} = -80, U_{10} = -20, m_0 = 0, m_1 = 0$ 5, and $\sigma_s^2 = 2.25$. In Fig. 2, we plot the optimal decision thresholds with respect to α , β under EUT and PT based subjective utility approaches. We also provide the optimal decision thresholds for PT based Bayesian formulation using numerical methods. It can be observed that under EUT, the decision threshold is a constant, without being affected by humans' behavioral properties. In this particular example, we can see that the decision thresholds, under both PT utility based methods and PT Bayesian methods, decrease as probability distortion parameter α decreases and decrease as loss aversion parameter β increases. An intuitive explanation for this is that as α decreases, the human perceives less distinction between the priors $\{\pi_0, \pi_1\}$. Therefore, the hypothesis with a smaller prior probability, in this case, H_1 , is more likely to be declared true and correspondingly, the decision threshold is decreasing. When β increases, the human perceives the penalty for miss detection $U_{01} = -80$ to be more significant than the penalty for false alarm $U_{10} = -20$. Therefore, the decision threshold is decreasing to avoid the possibility of miss detection.

In contrast to the fact that the Bayesian formulation is equivalent to the utility based decision making under EUT, there

exist disparities between these two approaches when PT is incorporated. Results in Fig. 2 suggest that when α is smaller and β is larger, the decision threshold under PT Bayesian formulation deviates more from the rational case than the decision threshold under PT utility based approaches. Note that when $\alpha=\beta=1$ and $\lambda=1$, i.e., the person is rational, the decision rule of both approaches reduces to the classical LRT (8).

The above results have provided us with the basic insights on how the parameters α and β from prospect theory affect the decision threshold used by a cognitively biased person in utility based decision making. We denote the cognitively biased threshold t as $t=\mathcal{F}(\alpha,\beta)$, where \mathcal{F} is monotone with respect to α and β .

D. Uncertainties in Human Decision Making

Unlike physical sensors, whose decision thresholds can be programmed to be fixed values that do not change, there are uncertainties in human decision making due to uncontrolled factors like time constraint, mood, environment, location and so on. Individual uncertainty (variability) is a prominent feature in human behavior. Variability is observed in human perception and decision making even when the external conditions, such as the sensory signals and the task environment, stay the same [31]. This is also known as trial-to-trial variability in psychology experiments, i.e., differences of responses are noticeable when the same experiment is repeated using the same human subject. From a psychology point of view, the sources of the variability are: a) the initial condition of the neural circuitry is likely to be different at the start of each trial, and b) the noise permeating in every level of the nervous system, from the perception of input observations to the stage of decision making. These two sources cause uncertainties in human decision making and are highly dependent on factors such as time constraints, outside environment and human mood [9], [32].

In the following, decision thresholds of humans are modeled as random variables as in [13], [18], [19]. Specifically, we model the threshold of a human to be $\tau = \mathcal{F}(\alpha, \beta) + v$, where $v \sim \mathcal{N}(0, \sigma_{\tau}^2)$. Here σ_{τ}^2 represents the variance associated with an agent while making a decision due to uncertainty as discussed above. From now on, we let τ denote the behaviorally biased decision threshold used by the human agent. τ is assumed to be a Gaussian random variable, whose mean is affected by the average level of human cognitive biases and the variance σ_{τ}^2 is due to decision uncertainties. A larger value of σ_{τ}^2 indicates higher uncertainty of a person while making a decision. To measure the individual uncertainty in human decision threshold, one may conduct the experiments as in [26] on the same human under different environments, e.g., time pressure, change of location, etc. In each experiment, the set of behavioral parameters α , β and λ of the human can be estimated. Since the variability of these parameters can be incorporated via the variability of the decision threshold, we can obtain the variance of the decision threshold by analyzing the statistics.

Lemma 1: In solving the hypothesis testing problem (13), if a human employs a random decision threshold $\tau \sim \mathcal{N}(m_{\tau}, \sigma_{\tau}^2)$,

the probabilities of false alarm and detection are given by

$$P_F = Q\left(\frac{m_{\tau} - m_0}{\sqrt{\sigma_s^2 + \sigma_{\tau}^2}}\right), \quad P_D = Q\left(\frac{m_{\tau} - m_1}{\sqrt{\sigma_s^2 + \sigma_{\tau}^2}}\right), \quad (14)$$

where Q(x) is the probability that a standard normal random variable takes a value larger than x: $Q(x) = \frac{1}{\sqrt{2\pi}} \int_x^{\infty} \exp\left(-\frac{u^2}{2}\right) du$.

Proof: See Appendix B.

Next, we want to study the impact of decision uncertainty quantified in terms of σ_{τ}^2 on human decision making performance. For a human agent who uses a random decision threshold $\tau \sim \mathcal{N}(m_{\tau}, \sigma_{\tau}^2)$ to make a decision in the binary hypothesis testing problem (13), we have the following theorem.

Theorem 2: There exists a pair of values $\{\underline{m}_{\tau}, \overline{m}_{\tau}\}$ where $\underline{m}_{\tau} < \overline{m}_{\tau}$ and both \underline{m}_{τ} and \overline{m}_{τ} satisfy:

$$e^{\frac{2(m_1 - m_0)m_\tau - (m_1^2 - m_0^2)}{2\sigma_s^2}} \times \left(\frac{m_\tau - m_1}{m_\tau - m_0}\right) = \eta,$$

such that for humans with $\underline{m}_{\tau} \leq m_{\tau} \leq \overline{m}_{\tau}$, the expected utility while making a decision monotonically decreases as σ_{τ}^2 becomes larger, i.e., the expected utility while making a decision is maximized for decision uncertainty $\sigma_t^{2^*} = 0$. For humans with $m_{\tau} > \overline{m}_{\tau}$ and $m_{\tau} < \underline{m}_{\tau}$, the expected utility is unimodal, i.e, first increases then decreases, as σ_{τ}^2 becomes larger. The optimal decision uncertainty $\sigma_{\tau}^{2^*}$ is greater than 0 and satisfies:

$$e^{\frac{2(m_1-m_0)m_{\tau}-(m_1^2-m_0^2)}{2(\sigma_s^2+{\sigma_{\tau}^2}^*)}}\times \left(\frac{m_{\tau}-m_1}{m_{\tau}-m_0}\right)=\eta.$$

Proof: See Appendix C.

Definition 1: Under the hypothesis testing framework discussed above, if for decision variance $\sigma_{\tau}^{2^*}=0$, a human obtains the maximum expected utility while making a decision and the expected utility decreases monotonically as σ_{τ}^2 increases, i.e, $\underline{m}_{\tau} \leq m_{\tau} \leq \overline{m}_{\tau}$, the person is called *reasonable*. If the best decision in terms of expected utility is made for decision variance $\sigma_{\tau}^{2^*}>0$, i.e., $m_{\tau}>\overline{m}_{\tau}$ or $m_{\tau}<\underline{m}_{\tau}$, the person is called **extremely biased**.

Some simulation results are provided when a human employs the decision threshold $\mathcal{N}(m_{\tau}, \sigma_{\tau}^2)$ in the hypothesis testing problem discussed before. In this case, we obtain that $\underline{m}_{\tau} = -0.025$ and $\overline{m}_{\tau} = 5.015$. Correspondingly, the left side extremely biased region, the reasonable region and the right side extremely biased region in terms of m_{τ} are $(-\infty, -0.025)$, [-0.025, 5.015] and $(5.015, \infty)$, respectively. In Fig. 3, we plot the expected utility of a human while making a decision with respect to the uncertainty of decision threshold σ_{τ}^2 . It can be observed that the expected utility of a reasonable human is monotonically decreasing with respect to σ_{τ}^2 . For extremely biased human agents, there exists an optimal value of decision uncertainty σ_{τ}^{2*} at which they achieve the maximum expected utility. Note that in this hypothesis testing problem, left side extremely biased humans whose decision threshold is on the far left typically perform better than a right side extremely biased humans agent whose decision threshold is on the far right. This is because the penalty of miss detection ($U_{01} = -80$) dominates

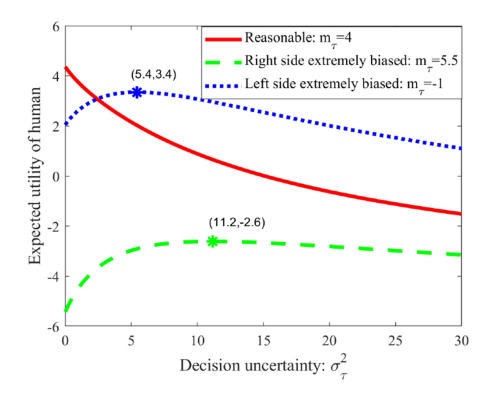


Fig. 3. Expected utility of a human agent as decision uncertainty σ_{τ}^2 increases.

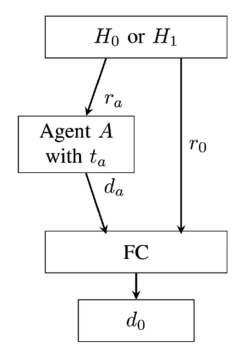


Fig. 4. Human participating in decision making as an assistant.

the penalty of false alarm $(U_{10}=-20)$ in this particular problem. Right side extremely biased humans with higher biased decision thresholds are more probable to suffer miss detection and their performance is significantly deteriorated. Moreover, it is observed in Fig. 3 that a left side extremely biased human outperforms a reasonable human after a certain value of σ_{τ}^2 is reached. The reason is that as the decision threshold variance σ_{τ}^2 increases, a reasonable human agent is more likely to employ higher biased decision thresholds than a left side extremely biased human, while degrading the performance due to higher cost of miss detection.

Remark: Extremely biased humans have their decision making performance enhanced in the presence of decision uncertainty up to a certain point before it begins to deteriorate. This is analogous to noise-enhanced signal processing [33] where the performance of a suboptimal detector can sometimes be enhanced by adding noise. This phenomenon is also known as stochastic resonance in the literature [34]–[36].

III. DECISION FUSION INVOLVING HUMAN PARTICIPATION

In this section, we analyze how the biased decision threshold τ employed by humans affects the performance of the decision making system in three different scenarios.

A. Human Participates in Decision Making as an Assistant, FC Is Rational

First, as shown in Fig. 4, we consider the scenario where a human agent assists the FC in making the final decision with the FC being rational (unbiased).

We assume that the FC observes r_0 and agent A observes r_a via orthogonal observation channels. The observation channels of both the FC and agent A are assumed to be corrupted by additive Gaussian noises, which are independent of each other but have the same PDF. The observations at the FC and agent A are denoted by r_0 and r_a to emphasize the fact that they are observed over two independent channels. Specifically, agent A is a human who makes a decision on which hypothesis is true by comparing r_a with a threshold t_a :

$$d_a = \begin{cases} 1 & \text{if } r_a \ge t_a \\ 0 & \text{if } r_a < t_a \end{cases}$$

For simplicity of exposition, we first consider t_a to be a fixed decision threshold determined by the PT parameters α_a and β_a , $t_a = \mathcal{F}(\alpha_a, \beta_a)$. Decision making uncertainty of agent A will be incorporated later in this subsection. After agent A sends its decision $d_a = j \in \{0,1\}$ to the FC, the FC makes the final decision d_0 based on d_a and its own observation r_0 . Given d_a and r_0 , the expected utilities for the FC to declare H_0 and H_1 are:

$$\begin{aligned} \mathbf{EU}(\text{Declare } H_0) &= \Pr(H_0|r_0, d_a = j) \\ U_{00} &+ \Pr(H_1|r_0, d_a = j) U_{01} \\ \mathbf{EU}(\text{Declare } H_1) &= \Pr(H_0|r_0, d_a = j) \\ U_{10} &+ \Pr(H_1|r_0, d_a = j) U_{11}, \end{aligned}$$

respectively. Choosing the hypothesis that has the larger expected utility yields the decision rule as:

$$\frac{\Pr(H_1|r_0, d_a = j)}{\Pr(H_0|r_0, d_a = j)} \stackrel{H_1}{\underset{H_0}{\geq}} \frac{U_{10} - U_{00}}{U_{01} - U_{11}},$$

where $Pr(H_i|r_0, d_a = j)$ represents the probability that H_i is true given observation r_0 and $d_a = j$. We have

$$\Pr(H_i|r_0, d_a = j) = \frac{\pi_i \Pr(d_a = j|H_i) f(r_0|H_i)}{f(r_0, d_a = j)}$$

for $i, j \in \{0, 1\}$. Note that $\Pr(d_a = 1|H_0) = P_F^a$, and $\Pr(d_a = 1|H_1) = P_D^a$, which are the probabilities of false alarm and detection of agent A, respectively. After simplification, the decision rule at the FC becomes:

$$\frac{f_1(r_0)}{f_0(r_0)} \underset{H_0}{\overset{H_1}{\geq}} \frac{1 - P_F^a}{1 - P_D^a} \frac{\pi_0(U_{10} - U_{00})}{\pi_1(U_{01} - U_{11})} = \frac{1 - P_F^a}{1 - P_D^a} \eta, \text{ if } d_a = 0,$$
(15)

$$\frac{f_1(r_0)}{f_0(r_0)} \stackrel{H_1}{\underset{H_0}{\geq}} \frac{P_F^a}{P_D^a} \frac{\pi_0(U_{10} - U_{00})}{\pi_1(U_{01} - U_{11})} = \frac{P_F^a}{P_D^a} \eta, \text{ if } d_a = 1.$$
 (16)

By setting $\frac{f_1(r_0)}{f_0(r_0)}=\frac{1-P_F^a}{1-P_D^a}\eta$ for $d_a=0$, and $\frac{f_1(r_0)}{f_0(r_0)}=\frac{P_F^a}{P_D^a}\eta$ for $d_a=1$, we obtain the decision thresholds applicable to observation r_0 at the FC, denoted by t_0 and t_1 , respectively. When observations under both hypotheses follow Gaussian distributions (13), we have $P_F^a=Q(\frac{t_a-m_0}{\sigma_s})$ and $P_D^a=Q(\frac{t_a-m_1}{\sigma_s})$. Considering the two scenarios together where $d_a=\{0,1\}$, the probability of false alarm and the probability of detection at the

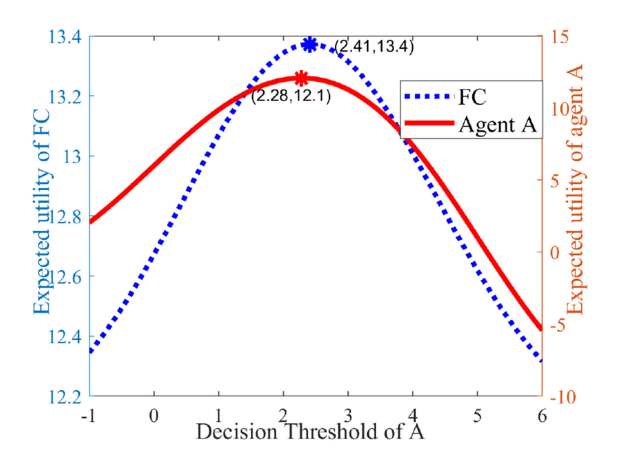


Fig. 5. Expected utility as a function of threshold t_a used by agent A.

FC can be expressed as:

$$\begin{split} p_f &= \sum_{j=0}^1 \Pr(d_0 = 1 | d_a = j, H_0) \Pr(d_a = j | H_0) \\ &= P_F^a Q\left(\frac{t_1 - m_0}{\sigma_s}\right) + (1 - P_F^a) Q\left(\frac{t_0 - m_0}{\sigma_s}\right), \\ p_d &= \sum_{j=0}^1 \Pr(d_0 = 1 | d_a = j, H_1) \Pr(d_a = j | H_1) \\ &= P_D^a Q\left(\frac{t_1 - m_1}{\sigma_s}\right) + (1 - P_D^a) Q\left(\frac{t_0 - m_1}{\sigma_s}\right), \end{split}$$

respectively. Then, the expected utility at the FC is:

$$U = \pi_0(1 - p_f)U_{00} + \pi_0 p_f U_{10} + \pi_1(1 - p_d)U_{01} + \pi_1 p_d U_{11}.$$
(17)

We conduct simulations for the same hypothesis testing problem as described in Section II-C. In Fig. 5, when agent A's decision threshold t_a varies, i.e., the cognitive bias of the human varies, we present the expected utilities of agent A by itself and that of the FC. Note that the thresholds used at agent A that yield the maximum expected utility for agent A by itself and that at the fusion center are different. In other words, a rationally behaving person who acts to maximize his/her EU (with decision threshold equal to 2.28 indicated by the red dot) does not necessarily provide the best performance for the FC. In this particular example, a person behaving with some biases (with decision threshold equal to 2.41 indicated by the blue dot) results in a larger expected utility for the FC. How to choose the properly biased person is dependent on the specific setup of the hypothesis testing problem. After knowing the effect of agent A's decision threshold on the FC's performance, we are able to determine a particular type of cognitively biased person, in terms of α , β , to be chosen to undertake the task.

Next, to incorporate decision making uncertainty, the decision threshold employed by agent A is considered to be a Gaussian random variable $\tau_a \sim \mathcal{N}(m_{\tau_a}, \sigma_{\tau_a}^2)$. In this case, P_F^a and P_D^a can be calculated through (14), and the optimal decision rule at the FC can be obtained in a manner similar to the previous discussions. The FC's expected utility can be correspondingly

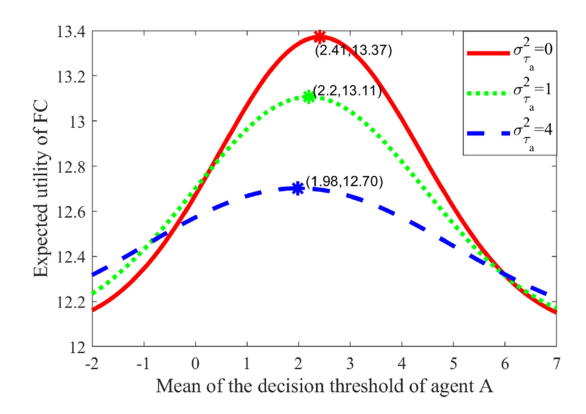


Fig. 6. Expected utility of the FC as a function of the mean threshold of agent A.

derived. In the following, we focus on studying the FC's decision making performance when the uncertainty of agent A's decision threshold changes.

With the earlier setup of the hypothesis testing problem, Fig. 6 shows the expected utility at the FC with respect to the mean decision threshold of agent A. In the red, green and blue curves, the variances of agent A's decision threshold are $\sigma_{\tau_a}^2 = 0$, $\sigma_{\tau_a}^2=1$ and $\sigma_{\tau_a}^2=4$, respectively. It is not surprising that the red curve with smallest decision making uncertainty performs better than the other two curves in the middle range of m_{τ_a} , namely when the human agents are reasonable. Thus, it is preferable to have human agents who are reasonable in that they are more predictable in the presence of decision making uncertainty and their performance degrades in a graceful manner. On the far left or far right of the graph, i.e., when the behavioral threshold is extremely biased, a larger variance surprisingly gives better performance at the FC. Intuitively, for extremely biased agents whose behavioral thresholds are far from being rational, a large variance is more likely to 'rectify' their thresholds to be close to optimal thresholds. However, for rational agents whose behavioral thresholds are already close to the optimal, a large variance is more likely to deviate their thresholds away from their optimal values. For this reason, a large variance helps increase the FC's utility when the agent is extremely biased, while it hurts when the agent is already behaving rationally. This phenomenon is consistent with our previous analysis about the effect of uncertainty on the quality of a single human agent's decision shown in Fig. 3.

Also notice that in Fig. 5, in order for the FC to derive maximum expected utility, agent A employed the fixed decision threshold $t_a=2.41$. When we introduce uncertainty in the decision threshold of agent A by increasing the variance in Fig. 6, the optimal mean of A's decision threshold while assisting FC to derive the largest expected utility, changes to $m_{\tau_a}=2.2$ when $\sigma_{\tau_a}^2=1$, and $m_{\tau_a}=1.98$ when $\sigma_{\tau_a}^2=4$. This is because with the same mean threshold m_{τ_a} , different variances result in different values of probability of false alarm and detection for agent A (as shown in (14)), which in turn leads to different decision thresholds used by the FC (calculated using (15) and (16)). Thus, the utility of the FC correspondingly changes. For this reason, we should also take the variance of the agent into

consideration when deciding the agent's optimal mean threshold while assisting the FC.

B. Human Is the Decision Maker at the FC, FC Is Biased

For the system shown in Fig. 4, next consider that A is a physical sensor with fixed decision threshold t_a . The FC is a biased human with behavioral parameters α , β and decision making uncertainty σ_{FC}^2 . Again, physical sensor A sends its decisions $d_a = j \in \{0,1\}$ to help the FC make the final decision. If the FC is biased, we need to apply $v(\cdot)$ and $w(\cdot)$ when calculating the FC's subjective utility of declaring either H_0 or H_1 being true, when agent A sends its decision $d_a = j$:

$$\mathbf{SU}(\text{Declare } H_0) = w \left(\Pr(H_0 | r_0, d_a = j) \right) V_{00} + w \left(\Pr(H_1 | r_0, d_a = j) \right) V_{01}$$
(18)

and

$$SU(Declare H_1)) = w \left(Pr(H_0|r_0, d_a = j) \right) V_{10} + w \left(Pr(H_1|r_0, d_a = j) \right) V_{11}.$$
(19)

The FC makes its decision by selecting the hypothesis which results in a higher subjective utility. Since the FC observes r_0 and agent A makes its decision independently, the likelihood ratio at the FC can be shown to be strictly increasing or decreasing with respect to observation r_0 . Hence, the FC uses a threshold based decision rule and the mean of the decision threshold m_{FC}^j is obtained by setting (18) equal to (19) for j=0,1. Finally, we model the decision threshold that the FC uses as a Gaussian random variable $\tau_0=\mathcal{N}(m_{FC}^j,\sigma_{FC}^2)$ to make the final decision, after it observes the decision made by agent A, $d_a=j$.

The probability of false alarm and probability of detection at the FC are:

$$\begin{split} p_f &= \sum_{j=0}^1 \Pr(d_0 = 1 | d_a = j, H_0) \Pr(d_a = j | H_0) \\ &= Q\left(\frac{t_a - m_0}{\sigma_s}\right) Q\left(\frac{m_{FC}^1 - m_0}{\sqrt{\sigma_s^2 + \sigma_{FC}^2}}\right) \\ &+ \left(1 - Q\left(\frac{t_a - m_0}{\sigma_s}\right)\right) Q\left(\frac{m_{FC}^0 - m_0}{\sqrt{\sigma_s^2 + \sigma_{FC}^2}}\right) \end{split}$$

and

$$\begin{split} p_d &= \sum_{j=0}^{1} \Pr(d_0 = 1 | d_a = j, H_1) \Pr(d_a = j | H_1) \\ &= Q\left(\frac{t_a - m_1}{\sigma_s}\right) Q\left(\frac{m_{FC}^1 - m_1}{\sqrt{\sigma_s^2 + \sigma_{FC}^2}}\right) \\ &+ \left(1 - Q\left(\frac{t_a - m_1}{\sigma_s}\right)\right) Q\left(\frac{m_{FC}^0 - m_1}{\sqrt{\sigma_s^2 + \sigma_{FC}^2}}\right), \end{split}$$

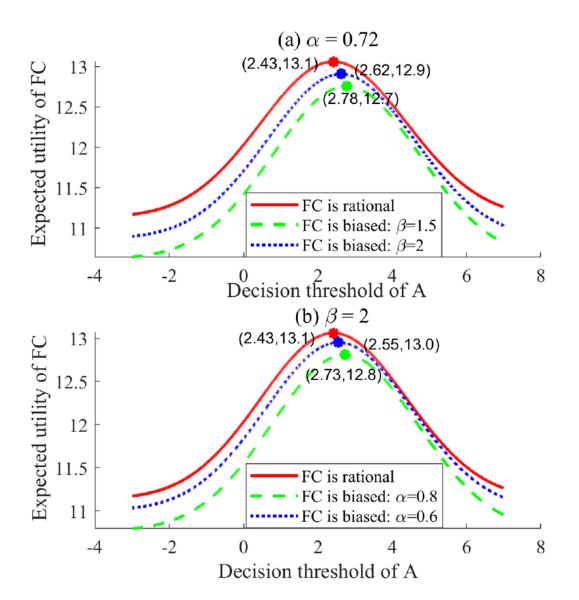


Fig. 7. Expected utility of FC as a function of the decision threshold of agent A, when FC has behavioral biases.

where $\Pr(d_0 = 1 | d_a = j, H_i) = Q(\frac{m_{FC}^j - m_i}{\sqrt{\sigma_s^2 + \sigma_{FC}^2}})$ for $i, j = \{0, 1\}$ follows directly from the result of Lemma 1. Again, the expected utility of FC can be calculated using (17).

Fig. 7 shows the expected utility of the FC with respect to the decision threshold t_a used by the physical sensor A. In Fig. 7(a), the red curve represents the scenario where the FC is rational, and in the green and blue curves the FC is behaviorally biased with $\beta = 1.5$ and $\beta = 2$, respectively. When the FC is biased, we set the FC's probability distortion parameter to be $\alpha = 0.72$. It is observed that the FC achieves higher expected utility when it acts rationally. On the other hand, the peak points on these curves (denoted by the red, green and blue dots) suggest that for FCs with different behavioral properties, the optimal decision threshold of A in helping the FC achieve the best utility differs. In such a decision making system where we are dealing with humans that do not provide an opportunity for parameter tuning while they make decisions, the best we can do is to acknowledge the fact that humans have cognitive biases and are subject to uncertainties and try to develop efficient approaches to optimize the system performance. In the problem considered here, we are tuning the threshold of the physical sensor A so as to help the FC/human optimize the decision quality.

Another interesting fact is that in this decision making configuration, a more biased behaving FC (indicated by the blue curve which has a larger β) outperforms a less biased FC (indicated by the green curve which has a smaller β) for the entire range of A's decision threshold. The reason is that under the joint influence of behavioral parameters α , β and γ , the threshold of the likelihood ratio test used by a biased FC deviates from the threshold used by a rational FC. In our case, a larger β counteracts the effect of α and γ , making the threshold used by the biased FC closer to that of a rational FC. In Fig. 7(b), we set the loss aversion parameter $\beta=2$ and plot the expected utility of the FC with respect to t_a as α varies. Similarly to the phenomenon in Fig. 7(a), it can be seen that a more biased value of $\alpha=0.6$ helps the FC make better

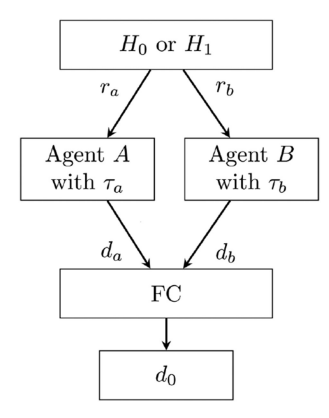


Fig. 8. Fusion of decisions made by two human agents.

decisions than $\alpha=0.8$ when $\beta=2$. In general, it is not wise to judge the decision making performance of a human based on the comparison of one single behavioral parameter, instead all the parameters should be treated together in a more holistic manner.

C. Fusion of Decisions Made by Two Human Agents

Now, consider the decision fusion scheme shown in Fig. 8, where A and B are two human agents that make local decisions d_a and d_b , which are transmitted to an unbiased FC to make the final decision. Let the decision threshold of A be $\tau_a \sim \mathcal{N}(m_{\tau_a}, \sigma_{\tau_a}^2)$, and the decision threshold of B be $\tau_b \sim \mathcal{N}(m_{\tau_b}, \sigma_{\tau_b}^2)$. Suppose the FC receives the decision $d_a = i \in \{0,1\}$ from agent A, and decision $d_b = j \in \{0,1\}$ from agent B. The expected utility of declaring H_1 and H_0 for a rational FC are:

$$EU(\text{Declare }H_0)$$
 = $\Pr(H_0|d_a=i,d_b=j)U_{00} + \Pr(H_1|d_a=i,d_b=j)U_{01}$
$$EU(\text{Declare }H_1)$$

=
$$\Pr(H_0|d_a = i, d_b = j)U_{10} + \Pr(H_1|d_a = i, d_b = j)U_{11}$$
.

The decision rule that declares the hypothesis which has the larger expected utility to be true, is

where $I(\cdot)$ is the indicator function which equals 1 if the statement inside the parentheses is true, and it equals 0 otherwise. The optimal decision rule of the FC requires the calculation of the probabilities of local decisions under hypotheses H_1 and H_0 , which depends on the decision thresholds used by the two human agents. Further, the probability of false alarm and detection at the FC are:

$$p_f = \sum_{i=0}^{1} \sum_{j=0}^{1} \Pr(d_0 = 1 | d_a = i, d_b = j) \Pr(d_a = i, d_b = j | H_0)$$

$$p_d = \sum_{i=0}^{1} \sum_{j=0}^{1} \Pr(d_0 = 1 | d_a = i, d_b = j) \Pr(d_a = i, d_b = j | H_1).$$

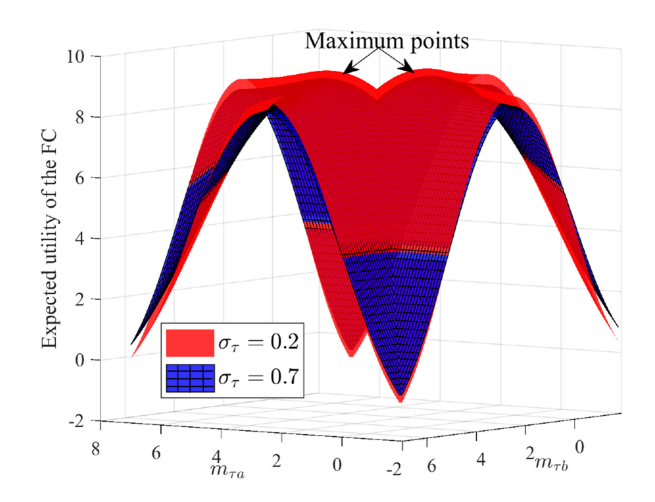


Fig. 9. Expected utility of the FC when fusing decisions of two human agents.

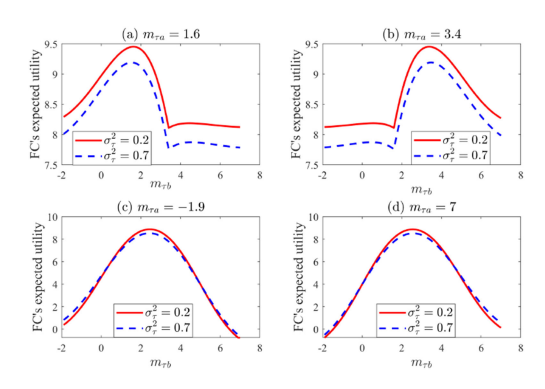


Fig. 10. FC's expected utility with respect to $m_{\tau b}$ for different values of $m_{\tau a}$.

Finally, the expected utility of the FC can be calculated using (17).

In Fig. 9, we plot the expected utility of the FC with respect to the mean values of the decision thresholds used by agents A and B, namely $m_{\tau a}$ and $m_{\tau b}$. In the red smooth surface, both agents have decision uncertainty $\sigma_{\tau}^2 = 0.2$, and in the blue meshed surface, both agents have decision uncertainty $\sigma_{\tau}^2 = 0.7$. In the graph, there are two local maximum points where the FC achieves locally optimal utilities. When the means of the decision thresholds deviate from their local maxima points, the utility drops significantly. We can also see that the agents with less decision making uncertainty (red curve) help the FC perform better than the agents with larger uncertainty do (blue curve) in the 'center' region of the graph. In the 'leaf' regions where humans are extremely biased, larger uncertainties produce higher utilities for the FC. For better visualization of the system performance, we present the cross section curves of Fig. 9 in Fig. 10, where we plot the FC's utility with respect to $m_{\tau b}$ for different values of $m_{\tau a}$. Fig. 10(a) and (b) correspond to the cross section plots yielding the two maximum utility points, respectively. Note that for both of the local maximal points, the mean value of the decision threshold of agent A is equal to that of agent B. In subplots Fig. 10(a) and (b) where the values of $m_{\tau a}$ are close to optimal, we observe that FC performs better when the value of σ_{τ}^2 is smaller. However, in subplots Fig. 10(c) and (d) where the values of $m_{\tau a}$ and $m_{\tau b}$ are both extremely biased, the blue curve with a larger decision uncertainty $\sigma_{\tau}^2=0.7$ outperforms red curve with a smaller decision uncertainty $\sigma_{\tau}^2=0.2$. This phenomenon coincides with what we observed in Fig. 6 when there was only one human participating.

IV. COLLABORATIVE DECISION MAKING

In this section, we consider the scenario where multiple human agents (n>2) participate in the collaborative decision making process. Each agent independently makes a decision $d_i \in \{0,1\}$ using a random decision threshold $\tau_i \sim \mathcal{N}(m_{\tau_i},\sigma_{\tau_i}^2)$, for $i=1,\ldots,n$. The FC receives a vector of decisions $D=\{d_1,\ldots,d_n\}$ and makes a final decision d_0 regarding the hypothesis present. As the number of agents becomes larger, the likelihood ratio test derived in the previous sections becomes complicated and intractable. However, if we know the behavioral property of each agent, we can derive the decision thresholds and calculate the probability of false alarm P_{F_i} and probability of detection P_{D_i} for each agent. The optimal fusion rule at the FC in this situation can be obtained by calculating the log likelihood ratio according to the Chair-Varshney rule [4] given as follows:

$$\log \frac{\Pr(H_1|D)}{\Pr(H_0|D)} = \log \frac{\pi_1}{\pi_0} + \sum_{s^+} \log \frac{P_{D_i}}{P_{F_i}} + \sum_{s^-} \log \frac{1 - P_{D_i}}{1 - P_{F_i}},$$

where s^+ represents the agents whose local decisions are 1 and s^- are agents with local decisions 0. Decisions are made based on:

$$\log \frac{\Pr(H_1|D)}{\Pr(H_0|D)} \overset{H_1}{\underset{H_0}{\geq}} \log \eta.$$

Another fusion rule that is widely used is the majority rule due to its simplicity even though it is not necessarily optimal. When the FC receives the decision vectors D, it calculates the sum of local decisions: $\Gamma = \sum_{i=1}^n d_i$. In the majority rule, the statistic Γ is compared to a preset threshold $k = \lceil n/2 \rceil$. If $\Gamma \geq k$, the FC decides that H_1 is true, otherwise the FC decides that H_0 to be true, i.e., $\Gamma \stackrel{>}{>}_{H_0}^{H_1} k$. In this case, $d_i \in \{0,1\}$ is a Bernoulli random variable with probability $\Pr(d_i = 1) = P_{D_i}$ under H_1 and $\Pr(d_i = 1) = P_{F_i}$ under H_0 . Thus, Γ is a Poisson Binomial distributed random variable. Under H_0 , for example, the probability mass function (PMF) of Γ is:

$$\Pr(\Gamma = \gamma) = \sum_{A \in F_{\gamma}} \prod_{i \in A} P_{F_i} \prod_{j \in A^c} (1 - P_{F_i}),$$

where F_{γ} is the set that contains all possible combinations of γ agents out of a total of n agents. The cardinality of F_{γ} is $\binom{n}{\gamma}$, so the computation becomes more complicated when n is large. In the following, we use the Binomial approximation as well as the normal approximation to estimate the statistics of Γ .

A. Approximations of p_d and p_f at the FC

Considering that the FC uses the majority rule, this subsection presents two approximation methods that allow us to compute

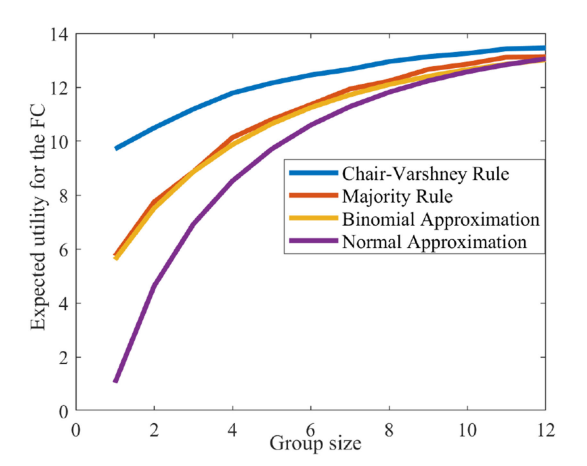


Fig. 11. Expected utility as a function of the group size.

the probabilities of false alarm and detection in a simpler and faster way.

- Binomial approximation: It can be seen that $\Pr(\Gamma) = \gamma$ approximately follows a Binomial PMF $B(n, \tilde{p}_f)$ under H_0 , where $\tilde{p}_f = \frac{1}{n} \sum_i^n P_{F_i}$, and it follows $B(n, \tilde{p}_d)$ under H_1 , where $\tilde{p}_d = \frac{1}{n} \sum_i^n P_{D_i}$. Thus, the probability of false alarm and the probability of detection at the FC can be approximated by $p_f = \Pr(d_0 = 1|H_0) \approx \sum_{\gamma=k}^n \binom{n}{\gamma} \tilde{p}_f^{\gamma} (1 \tilde{p}_f)^{n-\gamma}$ and $p_d = \Pr(d_0 = 1|H_1) \approx \sum_{\gamma=k}^n \binom{n}{\gamma} \tilde{p}_d^{\gamma} (1 \tilde{p}_d)^{n-\gamma}$, respectively.
 - Normal approximation: Since d_i s are independent, while not identically distributed Bernoulli random variables, we cannot use the central limit theorem (CLT) directly to approximate Γ to be Gaussian distributed when n is large. However, CLT can be generalized to be applied to independent but non-identically distributed random variables when the Lyapunov condition is satisfied: $\lim_{n\to\infty}\frac{1}{s_n^{2+\delta}}\sum_{i=1}^n E[|d_i-\mu_i|^{2+\delta}]=0,$ where $s_n = \sum_{i=1}^n \sigma_i^2$, μ_i and σ_i are the mean and standard deviation of each random variable. It is easy to verify that the Bernoulli random variables satisfy the Lyapunov condition. Therefore, when n is large, Γ can be approximated by a Gaussian random variable with mean $m_f = \sum_{i=1}^n P_{F_i}$ and variance $\sigma_f^2 = \sum_{i=1}^n P_{F_i} (1 - P_{F_i})$ under H_0 ; and mean $m_d = \sum_{i=1}^n P_{D_i}$ and variance $\sigma_d^2 = \sum_{i=1}^n P_{D_i} (1 - P_{D_i})$ under H_1 . Thus, the probabilities of false alarm and detection at the FC are approximated by $p_f = \Pr(d_0 =$ $1|H_0\rangle \approx \int_T^\infty \frac{1}{\sqrt{2\pi\sigma_f^2}} \exp\left(-\frac{(x-m_f)^2}{2\sigma_f^2}\right) dx = Q\left(\frac{T-m_f}{\sigma_f}\right),$ $p_d = \Pr(d_0 = 1|H_1) \approx \int_T^{\infty} \frac{1}{\sqrt{2\pi\sigma_d^2}} \exp(-\frac{(x-m_d)^2}{2\sigma_d^2}) dx =$ $Q(\frac{T-m_d}{\sigma_d})$, respectively.

With approximate values of p_f and p_d , the expected utility of the FC can be calculated via (17). Fig. 11 shows the expected utility of the FC as a function of group size when applying the Chair-Varshney decision rule, the majority rule, the Binomial and Gaussian approximations of the majority rule, respectively. In our simulation, the parameters of the hypothesis testing

problem are chosen to be the same as before, and each agent in the group has behavioral parameters $\alpha=0.72,~\beta$ is drawn from a Gaussian distribution $\mathcal{N}(m_\beta,\sigma_\beta^2)$, where $m_\beta=1.5$ and $\sigma_\beta^2=0.2$. The variance of human decision threshold is set equal to $\sigma_\tau^2=0.25$. Results are obtained through 5000 Monte Carlo trials. It is observed that the optimal Chair-Varshney decision rule outperforms the majority fusion rule. The expected utility of the FC under the majority rule goes up when the group size increases, and convergence occurs fairly fast. When the group size goes up to around 10, the performance reaches its saturation. We also observe that the binomial approximation method gives quite a good approximation to the majority rule and the Gaussian approximation starts to perform well when n becomes large as expected.

B. Optimal Decision Rule at the FC

In our previous analysis, the majority rule was used for decision fusion where the statistic Γ is compared to a threshold $k=\lceil n/2 \rceil$. The majority rule is a special case of the k out of n rule and is optimal only in certain scenarios. This rule is not necessarily optimal if the (binary) problem has non-uniform priors, non-uniform costs of false alarm and miss detection, non-identical local decision makers, etc. Here, we employ the more general k out of n rule, where $d_0=1$ is declared when k or more out of n people vote in favor of n rule so that the Bayesian utility at the FC is maximized. To characterize the local decision qualities, we use population-level averages of the probabilities of detection and false alarm, \hat{P}_D and \hat{P}_F , for each of the human agent.

Given that the sum of the local decisions is l, i.e., $\Gamma = l$, the expected utilities for the FC to declare H_0 and H_1 are:

$$EU(\text{Declare } H_0) = \Pr(H_0|\Gamma = l)U_{00} + \Pr(H_1|\Gamma = l)U_{01}$$

 $EU(\text{Declare } H_1) = \Pr(H_0|\Gamma = l)U_{10} + \Pr(H_1|\Gamma = l)U_{11},$

respectively, where $\Pr(H_i|\Gamma=l)=\frac{\pi_i\Pr(\Gamma=l|H_i)}{\Pr(\Gamma=l)}$ for $i=\{0,1\}$, and

$$\Pr(\Gamma = l | H_0) = \binom{n}{l} \hat{P}_F^l (1 - \hat{P}_F)^{n-l}$$

$$\Pr(\Gamma = l | H_1) = \binom{n}{l} \hat{P}_D^l (1 - \hat{P}_D)^{n-l}$$

respectively. The FC decides that hypothesis to be true which has a higher expected utility. After simplification, we obtain the optimal decision rule at the FC:

$$\left(\frac{\hat{P}_D}{\hat{P}_F}\right)^l \left(\frac{1-\hat{P}_D}{1-\hat{P}_F}\right)^{n-l} \stackrel{H_1}{\underset{H_0}{\geq}} \eta \tag{20}$$

where η is defined in (8). We make the reasonable assumption that $\hat{P}_D > \hat{P}_F$ [1], [27], so that the left hand side of (20) is an increasing function of l and the optimal decision rule reduces to $l \gtrsim^{H_1}_{H_0} l^*$, where the optimal threshold at the FC $k = l^*$ is the smallest integer l that satisfies $(\frac{\hat{P}_D}{\hat{P}_F})^l(\frac{1-\hat{P}_D}{1-\hat{P}_F})^{n-l} \geq \eta$.

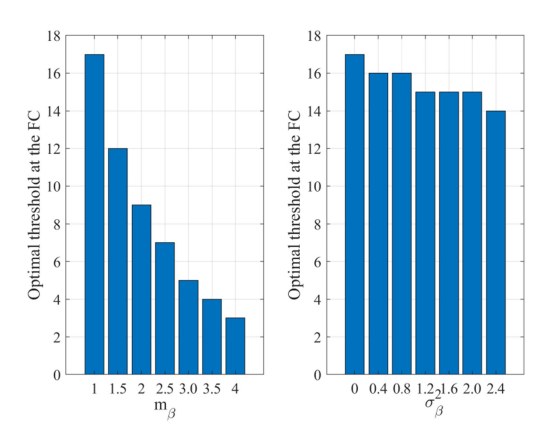


Fig. 12. Optimal threshold at the FC for different behavioral parameters of the group.

For a group size of n=20, we calculate the optimal threshold l^* for the k out of n rule when the behavioral properties of the people in the group change. In simulations, we set the group members' probability weight parameter α equal to 0.72, and let the loss aversion parameter β follow the Gaussian distribution $\mathcal{N}(m_\beta,\sigma_\beta^2)$, where m_β and σ_β^2 could change. We employ Monte Carlo methods to obtain the \hat{P}_D and \hat{P}_F of the agents numerically and calculate the optimal threshold l^* . In the left subplot of Fig. 12, we observe that with σ_β^2 fixed to be 0.25, the optimal threshold decreases when m_β increases. In the right subplot we set $m_\beta=2$, and it shows that the optimal threshold decreases as well when σ_β^2 becomes larger. Thus, it is important to understand the behavioral properties of the population in order to set the best threshold for the k out of n rule at the FC.

V. CONCLUSION

In this paper, we have explored the use of utility theory based hypothesis testing in human decision making. When humans are treated as rational agents who maximize their expected utilities, the results derived at the FC are not likely to be accurate. Humans have cognitive biases and make decisions so as to maximize their subjective utilities. The use of PT allows us to capture the non-rationality of humans. Specifically, we derived the subjective utility based decision rule for cognitively biased human agents modeled by PT. Three decision making systems involving humans' participation were explored, and we studied the impact of human behavioral biases on the quality of the final decisions. We also analyzed collaborative decision making and investigated the optimal k out of n rule at the FC while considering the behavioral biases of the participants.

This work is able to reveal fundamental features of human decision making under behavioral biases, as well as the significant differences between decision fusion involving human participants and information fusion with only physics-based sensors. Through the simple decision making systems discussed in this paper, we provided insights into the optimum design and task allocation of collaborative human-machine networks, as well as the development of more complicated human-centric intelligent systems. It will be worthwhile to study the optimal decision making architecture for particular applications in future work. We also plan to study the correlation among parameters

that represent different aspects of behavioral biases, and design applicable strategies to help human rectify the behavioral biases so as to make higher quality decisions.

Appendix A

We have already shown that the perceived utility decision rule under PT reduces to a LRT. To show that the threshold of the LRT, η_p , is monotone with respect to α , we take the derivative of the expression of η_p given in (12) with respect to α : $\frac{d}{d\alpha}\eta_{p} = \frac{-1}{\alpha^{2}} \frac{\pi_{0}}{\pi_{1}} \left(\frac{V_{00} - V_{10}}{V_{11} - V_{01}}\right)^{\frac{1}{\alpha}} ln(\frac{V_{00} - V_{10}}{V_{11} - V_{01}}). \text{ Since } \frac{-1}{\alpha^{2}} \frac{\pi_{0}}{\pi_{1}} \left(\frac{V_{00} - V_{10}}{V_{11} - V_{01}}\right)^{\frac{1}{\alpha}} is strictly negative, \frac{d}{d\alpha}\eta_{p} is always non-positive or non-negative$ depending on the sign of $ln(\frac{V_{00}-V_{10}}{V_{11}-V_{01}})$.

Similarly, differentiating η_p with respect to β , we get $\frac{d}{d\beta}\eta_p$ = $\frac{\pi_0}{\alpha \pi_1} \left(\frac{V_{00} - V_{10}}{V_{11} - V_{01}} \right)^{\frac{1}{\alpha} - 1} \frac{U_{11}^{\lambda} (-U_{10})^{\lambda} - U_{00}^{\lambda} (-U_{01})^{\lambda}}{(U_{11}^{\lambda} + \beta (-U_{01})^{\lambda})^2}, \text{ which is non-positive}$ or non-negative depending on the sign of $U_{11}^{\lambda}(-U_{10})^{\lambda}$ – $U_{00}^{\lambda}(-U_{01})^{\lambda}$, since all other terms are strictly positive. Thus, the likelihood ratio is monotone with respect to parameters α and β .

In the special case of $V_{00}-V_{10}=V_{11}-V_{01},\ \eta_p$ does not change when α varies; and in the special case of $U_{11}U_{10} =$ $U_{00}U_{10}$, η_p remains constant when β varies.

APPENDIX B

We write

$$P_D = \int_{-\infty}^{\infty} Pr(r \ge x | H_1) f_{\tau}(x) dx$$

$$= \int_{-\infty}^{\infty} Q\left(\frac{x - m_1}{\sigma_s}\right) \frac{1}{\sqrt{2\pi\sigma_{\tau}^2}} e^{\left(-\frac{(x - m_{\tau})^2}{2\sigma_{\tau}^2}\right)} dx \qquad (21)$$

Construct two independent random variables $X \sim \mathcal{N}(m_{\tau}, \sigma_{\tau}^2)$ and $Y \sim \mathcal{N}(0, \sigma_s^2)$. Since $X + Y \sim \mathcal{N}(m_\tau, \sigma_s^2 + \sigma_\tau^2)$, which is the same as the distribution of $Z + m_{\tau}$, where $Z \sim \mathcal{N}(0, \sigma_s^2 +$ σ_{τ}^2). Thus,

$$Pr(X + Y \le m_1) = Pr(Z \le m_1 - m_\tau)$$

$$= 1 - Q\left(\frac{m_1 - m_\tau}{\sqrt{\sigma_s^2 + \sigma_\tau^2}}\right) = Q\left(\frac{m_\tau - m_1}{\sqrt{\sigma_s^2 + \sigma_\tau^2}}\right). \tag{22}$$

where we use the fact that 1 - Q(x) = Q(-x). On the other hand, by the law of total probability (conditioning on X), we have:

$$Pr(X + Y \le m_1)$$

$$= \int_{-\infty}^{\infty} Pr(Y \le m_1 - x) \frac{1}{\sqrt{2\pi\sigma_{\tau}^2}} e^{\left(-\frac{(x - m_{\tau})^2}{2\sigma_{\tau}^2}\right)} dx$$

$$= \int_{-\infty}^{\infty} Q\left(\frac{x - m_1}{\sigma_s}\right) \frac{1}{\sqrt{2\pi\sigma_{\tau}^2}} e^{\left(-\frac{(x - m_{\tau})^2}{2\sigma_{\tau}^2}\right)} dx. \tag{23}$$

Observing that (23) is the same as the expression of p_d in (21), which in turn is equal to the expression in (22), it is easy to conclude that $P_D=Q(\frac{m_{ au}-m_1}{\sqrt{\sigma_s^2+\sigma_{ au}^2}}).$ Following a similar procedure, $P_F=Q(\frac{m_{\tau}-m_0}{\sqrt{\sigma_z^2+\sigma_z^2}})$ can be proved straightforwardly.

APPENDIX C

Following (17), we express the human's expected utility while making a decision:

$$U = \pi_0 U_{00} + \pi_1 U_{01} + \pi_1 (U_{11} - U_{01}) P_D - \pi_0 (U_{00} - U_{10}) P_F$$

$$\triangleq A P_D - B P_F + C,$$
(24)

where $A = \pi_1(U_{11} - U_{01})$, $B = \pi_0(U_{00} - U_{10})$ are positive constants and $C = \pi_0 U_{00} + \pi_1 U_{01}$. P_D and P_F represent the detection and false alarm probabilities of humans as given in (14).

When $m_0 < m_\tau < m_1$, from the expression in (14) we can see that P_F increases and P_D decreases as σ_{τ}^2 becomes larger. Thus, the expected utility U is a decreasing function with respect

Next, we consider $m_{\tau} \geq m_1$. In this case, both P_F and P_D increase with respect to σ_{τ}^2 . We substitute the expression of P_D and P_F in (14) in (24) and take the derivative with respect to σ_{τ}^2 :

$$\begin{split} \frac{\partial U}{\partial \sigma_{\tau}^2} &= \frac{1}{2\sqrt{2\pi(\sigma_s^2 + \sigma_{\tau}^2)^3}} \\ &\times \left(e^{-\frac{(m_{\tau} - m_1)^2}{2(\sigma_s^2 + \sigma_{\tau}^2)}} (m_{\tau} - m_1)A - e^{-\frac{(m_{\tau} - m_0)^2}{2(\sigma_s^2 + \sigma_{\tau}^2)}} (m_{\tau} - m_0)B\right). \end{split}$$

It follows that $\frac{\partial U}{\partial \sigma^2} \geq 0$ if and only if

$$g \triangleq e^{\frac{2(m_1 - m_0)m_{\tau} - (m_1^2 - m_0^2)}{2(\sigma_s^2 + \sigma_{\tau}^2)}} \times \left(\frac{m_{\tau} - m_1}{m_{\tau} - m_0}\right) \ge \frac{B}{A},$$

where g is a function that decreases with respect to σ_{τ}^2 . When $g|_{\sigma_{\tau}^2=0} \leq \frac{B}{A}$, we have $\frac{\partial U}{\partial \sigma_{\tau}^2} \leq 0$ for all $\sigma_{\tau}^2 \geq 0$, which suggests that U is a decreasing function with respect to σ_{τ}^2 . When $g|_{\sigma_{\tau}^2=0}>\frac{B}{A}$, there exists a point σ_{τ}^{2*} such that $g|_{\sigma_{\tau}^2<\sigma_{\tau}^{2*}}>$ $\frac{B}{A}$, i.e., $\frac{\partial U}{\partial \sigma_x^2} > 0$; and $g|_{\sigma_\tau^2 < \sigma_\tau^{2^*}} \leq \frac{B}{A}$, i.e., $\frac{\partial U}{\partial \sigma_z^2} \leq 0$. In other words, U first increases and then decreases as σ_{τ}^2 becomes larger. The threshold σ_{τ}^{2*} is obtained by solving the equation

e arger. The threshold
$$\sigma_{\tau}$$
 is obtained by
$$e^{\frac{2(m_1 - m_0)m_{\tau} - (m_1^2 - m_0^2)}{2(\sigma_s^2 + \sigma_{\tau}^{2^*})}} \times (\frac{m_{\tau} - m_1}{m_{\tau} - m_0}) = \frac{B}{A}.$$
On the other hand, a is an increasing

On the other hand, g is an increasing function with respect to m_{τ} . Note that $g|_{m_{\tau}=m_1}=0$ and $g|_{m_{\tau}=\infty}=\infty$. Therefore, there exists a $\overline{m}_{\tau} > m_1$ such that $g|_{\sigma_{\tau}^2 = 0, m_{\tau} \leq \overline{m}_{\tau}} \leq \frac{B}{A}$ and $g|_{\sigma_{\tau}^2=0,m_{\tau}>\overline{m}_{\tau}}> rac{B}{A}.$ In other words, when $m_1\leq m_{\tau}\leq \overline{m}_{\tau}, U$ is a decreasing function with respect to σ_{τ}^2 and when $m_{\tau}>\overline{m}_{\tau}, U$

$$U$$
 is unimodal with respect to $\sigma_{ au}^2$. $\overline{m}_{ au}$ is obtained by solving $m_{ au}$ in the equation $e^{\frac{2(m_1-m_0)m_{ au}-(m_1^2-m_0^2)}{2\sigma_s^2}} imes (\frac{m_{ au}-m_1}{m_{ au}-m_0}) = \frac{B}{A} = \eta.$ The analysis of the case $m_{ au} < m_0$ is similar to the

above derivations. There exists a $\underline{m}_{\tau} < m_0$ such that Uis a decreasing function with respect to σ_{τ}^2 when $\underline{m}_{\tau} \leq$ $m_{\tau} \leq m_0$, and U is unimodal with respect to σ_{τ}^2 when $m_{\tau} < \underline{m}_{\tau}$. \underline{m}_{τ} is obtained by solving m_{τ} in the equation

$$e^{\frac{-2(m_1-m_0)m_{\tau}+(m_1^2-m_0^2)}{2\sigma_s^2}}\times (\frac{m_{\tau}-m_0}{m_{\tau}-m_1})=\frac{A}{B}=\frac{1}{\eta}, \text{ which is equivalent to } e^{\frac{2(m_1-m_0)m_{\tau}-(m_1^2-m_0^2)}{2\sigma_s^2}}\times (\frac{m_{\tau}-m_0}{m_{\tau}-m_1})=\eta.$$

REFERENCES

- P. K. Varshney, Distributed Detection and Data Fusion. Berlin, Germany: Springer Science & Business Media, 2012.
- [2] V. V. Veeravalli and P. K. Varshney, "Distributed inference in wireless sensor networks," *Philos. Trans. Royal Soc. A: Math., Physical Eng. Sci.*, vol. 370, no. 1958, pp. 100–117, 2012.
- [3] R. Viswanathan and P. K. Varshney, "Distributed detection with multiple sensors part I. Fundamentals," *IEEE Proc.*, vol. 85, no. 1, pp. 54–63, Jan. 1997.
- [4] Z. Chair and P. Varshney, "Optimal data fusion in multiple sensor detection systems," *IEEE Trans. Aeros. Electron. Syst.*, vol. AES-22, no. 1, pp. 98– 101, Jan. 1986.
- [5] M. Kam, Q. Zhu, and W. S. Gray, "Optimal data fusion of correlated local decisions in multiple sensor detection systems," *IEEE Trans. Aerosp. Electron. Syst.*, vol. 28, no. 3, pp. 916–920, Jul. 1992.
- [6] D. Kahneman and A. Tversky, "Prospect theory: An analysis of decision under risk," in *Handbook of the Fundamentals of Financial Decision Making: Part I.* Singapore: World Scientific, 2013, pp. 99–127.
- [7] H. J. Einhorn and R. M. Hogarth, "Behavioral decision theory: Processes of judgement and choice," *Annu. Rev. Psychol.*, vol. 32, no. 1, pp. 53–88, 1981.
- [8] N. Barberis and R. Thaler, "A survey of behavioral finance," Handbook of the Economics of Finance, vol. 1, pp. 1053–1128, 2003.
- [9] J. G. Johnson and J. R. Busemeyer, "Decision making under risk and uncertainty," Wiley Interdisciplinary Rev.: Cogn. Sci., vol. 1, no. 5, pp. 736–749, 2010.
- [10] F. H. Poletiek, Hypothesis-Testing Behaviour. Psychology Press, London U.K., 2013.
- [11] V. S. S. Nadendla, S. Brahma, and P. K. Varshney, "Towards the design of prospect-theory based human decision rules for hypothesis testing," in *Proc. 54th Annu. Allerton Conf. Commun., Control, Comput.*, Sep. 2016, pp. 766–773.
- [12] S. Gezici and P. K. Varshney, "On the optimality of likelihood ratio test for prospect theory based binary hypothesis testing," *IEEE Signal Process*. *Lett.*, vol. 25, no. 12, pp. 1845–1849, Dec. 2018.
- [13] R. D. Sorkin, R. West, and D. E. Robinson, "Group performance depends on the majority rule," *Psychological Sci.*, vol. 9, no. 6, pp. 456–463, 1998.
- [14] D. V. Budescu, A. K. Rantilla, H.-T. Yu, and T. M. Karelitz, "The effects of asymmetry among advisors on the aggregation of their opinions," *Organizational Behav. Human Decis. Processes*, vol. 90, no. 1, pp. 178–194, 2003
- [15] R. D. Sorkin, C. J. Hays, and R. West, "Signal-detection analysis of group decision making." *Psychological Rev.*, vol. 108, no. 1, 2001, Art. no. 183.
- [16] J. B. Rhim, L. R. Varshney, and V. K. Goyal, "Quantization of prior probabilities for collaborative distributed hypothesis testing," *IEEE Trans. Signal Process.*, vol. 60, no. 9, pp. 4537–4550, Sep. 2012.
- [17] A. Vempaty, L. R. Varshney, G. J. Koop, A. H. Criss, and P. K. Varshney, "Experiments and models for decision fusion by humans in inference networks," *IEEE Trans. Signal Process.*, vol. 66, no. 11, pp. 2960–2971, Jun. 2018.

- [18] T. Wimalajeewa and P. K. Varshney, "Collaborative human decision making with random local thresholds," *IEEE Trans. Signal Process.*, vol. 61, no. 11, pp. 2975–2989, Jun. 2013.
- [19] T. Wimalajeewa, P. K. Varshney, and M. Rangaswamy, "On integrating human decisions with physical sensors for binary decision making," in *Proc. IEEE 21st Int. Conf. Inf. Fusion (FUSION)*, 2018, pp. 1–5.
- [20] B. Geng, Q. Li, and P. K. Varshney, "Decision tree design for classification in crowdsourcing systems," in *Proc. 52nd Asilomar Conf. Signals, Syst. Comput.*, Oct. 2018, pp. 859–863.
- [21] S. Plous, The Psychology of Judgment and Decision Making. New York, NY, USA: Mcgraw-Hill Book Company, 1993.
- [22] W. Edwards, "The theory of decision making," Psychological Bull., vol. 51, no. 4, 1954, Art. no. 380.
- [23] J. A. Swets, W. P. Tanner Jr, and T. G. Birdsall, "Decision processes in perception." *Psychological Rev.*, vol. 68, no. 5, 1961, Art. no. 301.
- [24] J. B. Soll and R. P. Larrick, "Strategies for revising judgment: How (and how well) people use others opinions," J. Exp. Psychol.: Learn., Memory, Cognition, vol. 35, no. 3, 2009, Art. no. 780.
- [25] D. Tapscott and A. D. Williams, Wikinomics: How Mass Collaboration Changes Everything. Baltimore, MD, USA: Penguin, 2008.
- [26] A. Tversky and D. Kahneman, "Advances in prospect theory: Cumulative representation of uncertainty," *J. Risk Uncertainty*, vol. 5, no. 4, pp. 297–323, 1992.
- [27] S. M. Kay, Fundamentals of Statistical Signal Processing. Englewood Cliffs, NJ, USA: Prentice Hall PTR, 1993.
- [28] P. Mongin, "Expected utility theory," Handbook of Economic Methodology, vol. 342350, pp. 342–350, 1997.
- [29] F. S. Hillier, Introduction to Operations Research. New York, NY, USA: Tata McGraw-Hill Education, 2012.
- [30] E. Alpaydin, Introduction to Machine Learning. Cambridge, MA, USA: MIT Press, 2009.
- [31] R. Chaudhuri and I. Fiete, "Computational principles of memory," *Nature Neuroscience*, vol. 19, no. 3, 2016, Art. no. 394.
- [32] A. A. Faisal, L. P. Selen, and D. M. Wolpert, "Noise in the nervous system," Nature Reviews Neurosci., vol. 9, no. 4, 2008, Art. no. 292.
- [33] H. Chen, L. R. Varshney, and P. K. Varshney, "Noise-enhanced information systems," *IEEE Proc.*, vol. 102, no. 10, pp. 1607–1621, Oct. 2014.
- [34] S. Kay, "Can detectability be improved by adding noise?" *IEEE Signal Process. Lett.*, vol. 7, no. 1, pp. 8–10, Jan. 2000.
- [35] H. Chen, P. K. Varshney, S. M. Kay, and J. H. Michels, "Theory of the stochastic resonance effect in signal detection—part I: Fixed detectors," *IEEE Trans. Signal Process.*, vol. 55, no. 7, pp. 3172–3184, Jul. 2007.
- [36] H. Chen and P. K. Varshney, "Theory of the stochastic resonance effect in signal detection—part II: Variable detectors," *IEEE Trans. Signal Process.*, vol. 56, no. 10, pp. 5031–5041, Oct. 2008.